Electronic Supplementary Material (ESI) for Nanoscale.

Supplementary information

Electrostatic crosslinking-enabled highly asymmetric lamellar nanostructure of polyzwitterionic block copolymers for lithography

Shi-Peng Ding, Ze-Kun Zhang, Ze Ye, Ding-Li Xia and Jun-Ting Xu*

State Key Laboratory of Motor Vehicle Biofuel Technology, International Research Center for X Polymers, Department of Polymer Science and Engineering, Zhejiang University, Hangzhou 310027, China

Contents:

---

* Corresponding author. E-mail: xujt@zju.edu.cn

Part 1: Synthesis and characterization of PS-*b*-PVPS BCPs

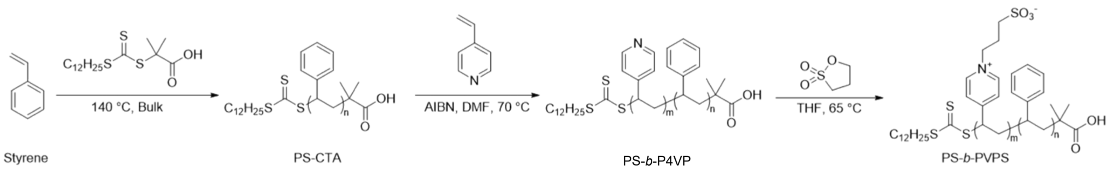

Fig. S1 Synthetic routine of PS-*b*-PVPS BCPs.

Synthesis and characterization of PS-CTAs

PS-CTAs were synthesized according to reference 1. To a Schlenk flask was added 2-(dodecylthiocarbonothioylthio)-2-methylpropionic acid and certain volume of styrene. After three freezing-degassing cycles, the flask was put in an oil bath preset at 140 °C and the reaction was stopped by liquid nitrogen after 6 h. The final solution was diluted with THF and precipitated into methanol for three times. The details of PS-CTAs are given in Table S1.

Table S1 Details of PS-CTAs

name	$Đ^a$	Mn^a_{GPC} (kg·mol^{-1})	Mn^b_{NMR} (kg·mol^{-1})
PS_{122}-CTA	1.05	13.0k	13.1k
PS_{102}-CTA	1.06	11.0k	11.0k
PS_{92}-CTA	1.06	9.9k	9.9k
PS_{82}-CTA	1.06	8.8k	8.9k
PS_{70}-CTA	1.07	7.7k	7.6k
PS_{67}-CTA	1.08	7.3k	7.3k
PS_{48}-CTA	1.07	5.0k	5.4k

[a]The polydispersity indexes ($Đ$) and number-average molecular weights (Mn_{GPC}) were determined by GPC with THF as eluent. [b]The average molecular weights (Mn_{NMR}) were calculated through ^{1}H NMR spectra.

Synthesis and characterization of PS-*b*-P4VP BCPs

To a Schlenk flask was added PS-CTA, 4-vinylpyridine, AIBN and DMF ([AIBN]: [CTA] = 0.2 : 1). After three freezing-degassing cycles, the flask was put in an oil bath preset at 70 °C and the reaction was stopped after 1 h. The final solution was poured into dialysis bags and dialyzed against THF for 24 h. PS-*b*-P4VP BCPs were collected by precipitation into *n*-hexane followed by centrifuge. The polymerization degree was calculated via ^{1}H NMR (Fig. S2). GPC traces of PS-*b*-P4VP BCPs are shown in Fig. S3. The details of PS-*b*-P4VP BCPs are given in Table S2.

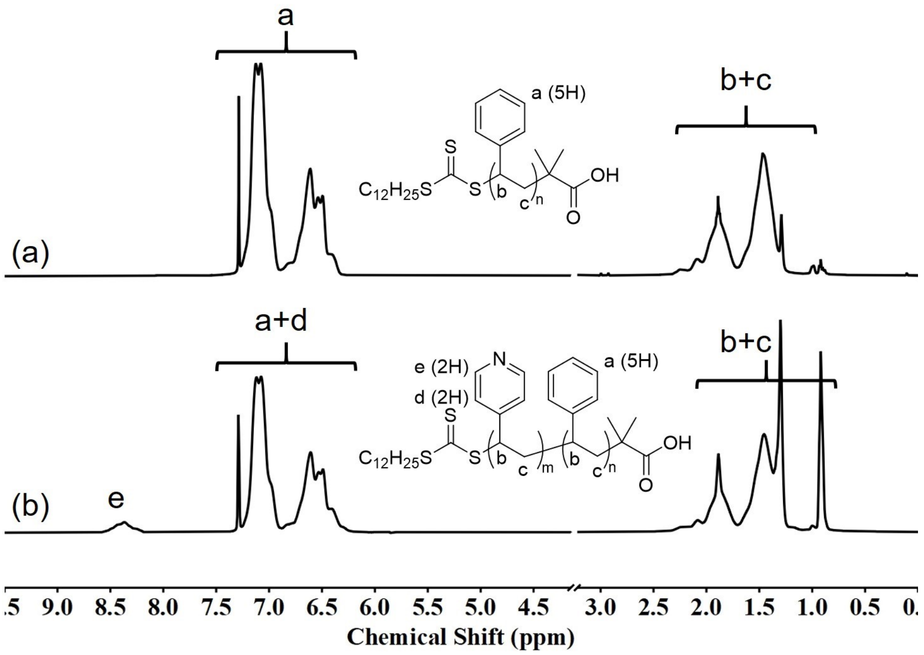

Fig. S2 Representative ^{1}H NMR spectra of PS_{122}-CTA (a) and $S_{122}4VP_{16}$ (b) in $CDCl_3$.

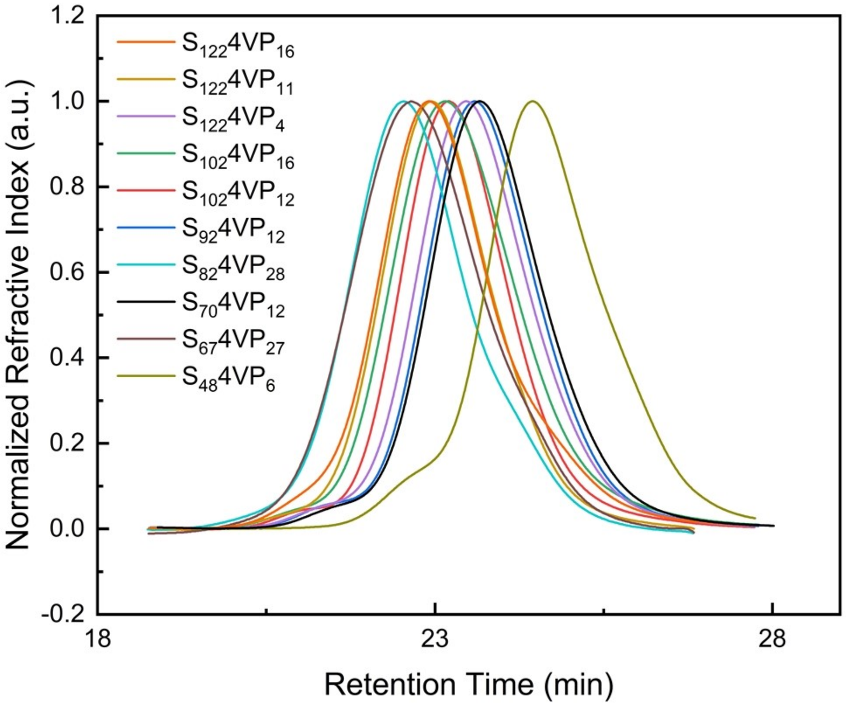

Fig. S3 GPC traces of PS-*b*-P4VP BCPs.

Table S2 Details of PS-*b*-P4VP BCPs

Samples	$M_n^{\mathrm{NMR}\ a}$ (kg·mol^{-1})	$Đ^b$
$S_{122}4VP_{16}$	14.4	1.12
$S_{122}4VP_{11}$	13.8	1.09
$S_{122}4VP_{4}$	13.1	1.09
$S_{102}4VP_{16}$	12.3	1.10
$S_{102}4VP_{12}$	11.9	1.10
$S_{92}4VP_{22}$	11.9	1.10
$S_{82}4VP_{28}$	11.5	1.12
$S_{70}4VP_{12}$	8.5	1.12
$S_{67}4VP_{27}$	9.8	1.13
$S_{48}4VP_{6}$	5.6	1.10

[a]The polymerization degrees (*DP*) of P4VP block and the molecular weights of BCPs were calculated from ^{1}H NMR spectra. [b]The polydispersity indexes (*Đ*) were determined by GPC with DMF as eluent.

Synthesis and characterization of PS-*b*-PVPS BCPs

To a round-bottom flask was added PS-*b*-P4VP, THF and 1,3-propanesultone (ten times the equivalent of 4VP unit) and the reaction was conducted at 65 °C for 24 h. The final solution was poured into dialysis bags and dialyzed against THF for 3 days. PS-*b*-PVPS products were collected by slowly evaporating the THF solution under ambient condition for more than one week followed by drying under vacuum. The modification of zwitterionic structure was proved by FTIR as indicated in Fig. S4. As indicated by FTIR spectra, the shift of the absorption of C=N bond from 1600 cm^{-1} to 1640 cm^{-1} and the shift of the absorption of C=C bond from 1420 cm^{-1} to 1470 cm^{-1} confirmed the quaternization of pyridine group. The appearance of the broad peak at ~1200 cm^{-1} (corresponding to the absorption of S=O bond) and the sharp peak at ~1040 cm^{-1} (corresponding to C-S bond) proved the formation of sulfonate group. Above characterization could confirm the formation of zwitterionic structure.

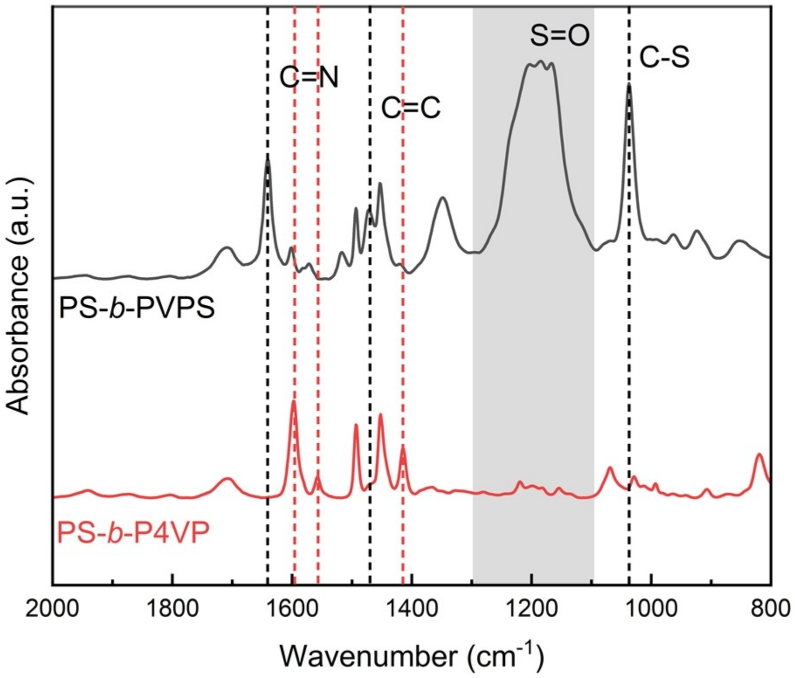

Fig. S4 FTIR spectra of PS-*b*-P4VP and PS-*b*-PVPS

Part 2: Morphologies of S$_x$VPS$_y$ BCPs

Table S3 Comparison of characteristics of A-LAM structure between SAXS and TEM results.

Samples	D (nm)		l_{PS} (nm)		l_{PVPS} (nm)		$l_{\mathrm{PS}} : l_{\mathrm{PVPS}}$	
	SAXS	TEM	SAXS, f	TEM	SAXS, f	TEM	f	TEM
$S_{122}VPS_{16}$	22.0	22.5	17.5	18.0	4.5	4.5	3.89	4.0
$S_{102}VPS_{16}$	21.3	21.5	16.3	16.5	5.0	5.0	3.26	3.3
$S_{102}VPS_{12}$	23.1	23.0	18.8	18.5	4.3	4.5	4.37	4.1
$S_{70}VPS_{12}$	17.0	17.5	12.7	13.0	4.3	4.5	2.95	2.9
$S_{48}VPS_{6}$	11.4	11.5	9.0	9.0	2.4	2.5	3.75	3.6

Fitting SAXS profile with a variable lamellar thickness structure model

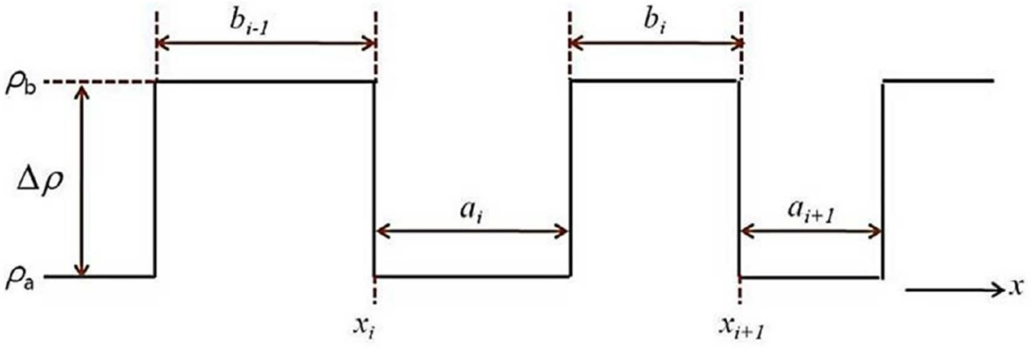

Fig. S5 Scattering length density profiles in the direction perpendicular to the lamellar plane for the variable lamellar thickness structure model.

The scattering length density profiles in the direction perpendicular to the lamellar plane for the variable lamellar thickness structure model is shown in Fig. S5. The thickness of the lamella changes more or less randomly from one to the next and there is no correlation between the thickness of neighboring lamella. The detail derivation of the model can be found in literature.[2] The conclusive formula can be expressed as

$$I(q) = 2N\left(\frac{\Delta\rho}{q}\right)^2 \frac{1}{(1-g_a g_b)^2 + 4 g_a g_b sin^2\left(\frac{qd}{2}\right)} \times [(1-g_a)(1-g_b)(1-g_a g_b) + 2g$$
$$sin^2\left(\frac{qd_a}{2}\right) + 2g_b\left(1-g_a^2\right) sin^2\left(\frac{qd_b}{2}\right)]$$

(S1)

Where $d = d_a + d_b$ and

$$g_a = e^{-\frac{1}{2}\sigma_a^2 q^2}, g_b = e^{-\frac{1}{2}\sigma_b^2 q^2} \qquad \text{(S2)}$$

$I(q)$ is the scattering intensity, q is the scattering vector, N is the number of lamella in the stack which is considered sufficiently large, d is the domain spacing, d_a and d_b are the thickness of two phases, respectively, σ_a and σ_b are the standard deviation of the thicknesses of A and B lamella, respectively.

For small values of σ_a and σ_b, Eqn. (1) can be estimated as follows:

$$I(q) = 16N\frac{(\Delta\rho)^2}{q^4} \frac{\sigma_b^2 sin^2(\frac{qd_a}{2}) + \sigma_a^2 sin^2(\frac{qd_b}{2})}{(\sigma_a^2 + \sigma_b^2) + \frac{16}{q^4} sin^2(\frac{qd}{2})} \qquad \text{(S3)}$$

Since $f = d_a/d$, Eqn. (3) can also be written as

$$I(q) = 16N\frac{(\Delta\rho)^2}{q^4} \frac{\sigma_b^2 sin^2(\frac{qfd}{2}) + \sigma_a^2 sin^2(\frac{q(1-f)d}{2})}{(\sigma_a^2 + \sigma_b^2) + \frac{16}{q^4} sin^2(\frac{qd}{2})} \qquad \text{(S4)}$$

After Lorentz correction, SAXS profiles can be fitted through Eq. (S4) and the parameters (f, σ_a and σ_b) can be acquired from the fitting results.

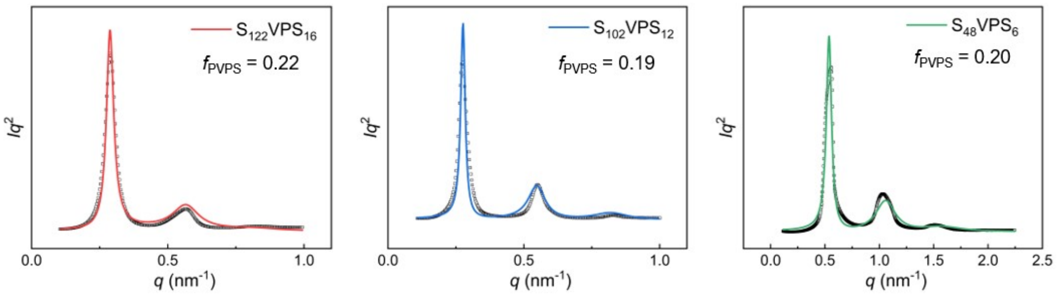

Fig. S6 Fitting results of the SAXS profiles. Open squares represent the experimental data and solid lines are the fitting results.

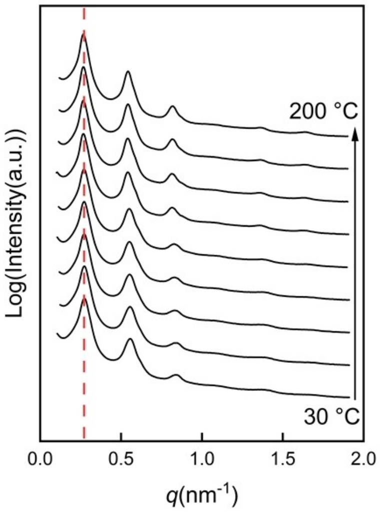

Fig. S7 Temperature-variable SAXS profiles of $S_{102}VPS_{12}$.

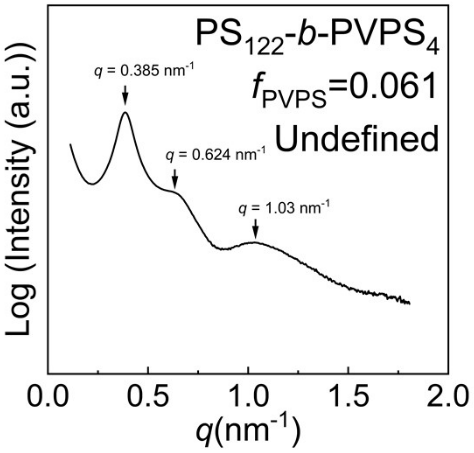

Fig. S8 SAXS profile of $S_{122}VPS_4$.

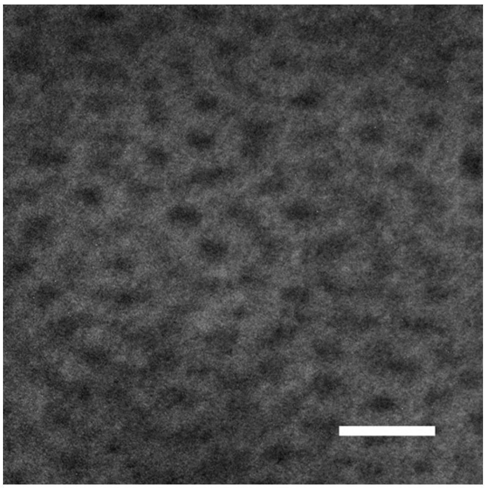

Fig. S9 TEM image of $S_{122}VPS_{11}$. The scale bar is 30 nm.

References

1 S. S. Zhang, K. Cui, J. Huang, Q. L. Zhao, S. K. Cao and Z. Ma, *RSC Adv.*, 2015, **5**, 44571-44577.

2 J. Kwak, S. H. Han, H. C. Moon and J. K. Kim, *Macromolecules*, 2015, **48**, 1262-1266.